

Why I'm not Answering: An Abstention Based Approach to Classify Cancer Pathology Reports

Sayera Dhaubhadel*, Jamaludin Mohd-Yusof*, Kumkum Ganguly*, Gopinath Chennupati*,

Sunil Thulasidasan*, Nicolas Hengartner*, Brent J. Mumphrey†, Eric B. Durban‡,

Jennifer A. Doherty§, Mireille Lemieux¶, Noah Schaefferkoetter||, Georgia Tourassi||,

Linda Coyle**, Lynne Penberthy††, Benjamin McMahon*, and Tanmoy Bhattacharya*

*Los Alamos National Laboratory, Los Alamos, NM 87545, USA,

†Louisiana Tumor Registry, New Orleans, LA 70122, USA,

‡Kentucky Cancer Registry, Lexington, KY 40504, USA,

§Utah Cancer Registry, Salt Lake City, UT 84112, USA,

¶New Jersey State Cancer Registry, New Brunswick, NJ 08903, USA,

||Oak Ridge National Laboratory, Oak Ridge, TN 37831, USA,

**Information Management Services Inc, Calverton, MD 20705, USA

††Division of Cancer Control and Population Sciences, National Cancer Institute, Bethesda, MD 20850, USA,

Abstract—Safe deployment of deep learning systems in critical real world applications requires models to make few mistakes, and only under predictable circumstances. Development of such a model is not yet possible, in general. In this work, we address this problem with an abstaining classifier tuned to have >95% accuracy, and identify the determinants of abstention with LIME (the Local Interpretable Model-agnostic Explanations method). Essentially, we are training our model to learn the attributes of pathology reports that are likely to lead to incorrect classifications, albeit at the cost of reduced sensitivity. We demonstrate our method in a multitask setting to classify cancer pathology reports from the NCI SEER cancer registries on six tasks of greatest importance. For these tasks, we reduce the classification error rate by factors of 2–5 by abstaining on 25–45% of the reports. For the specific case of cancer site, we are able to identify metastasis and reports involving lymph nodes as responsible for many of the classification mistakes, and that the extent and types of mistakes vary systematically with cancer site (eg. breast, lung, and prostate). When combining across three of the tasks, our model classifies 50% of the reports with an accuracy greater than 95% for three of the six tasks and greater than 85% for all six tasks on the retained samples. By using this information, we expect to define work flows that incorporate machine learning only in the areas where it is sufficiently robust and accurate, saving human attention to areas where it is required.

Availability: The data used in the analyses are health information legally protected against disclosure, and the property of the Louisiana, Kentucky, Utah, and New Jersey registries. Their use in the research has been approved by the appropriate authorities at the registries, the central DOE IRB, and the IRBs of the participating institutions.

I. INTRODUCTION

Real world deployed machine learning systems often encounter unforeseen situations not thoroughly explored during the model training. Such situations include data noise,

This work is funded by the Joint Design of Advanced Computing Solutions for Cancer program established by the US Department of Energy and the US National Cancer Institute.

variation in class composition, data quality, and site-specific and time-dependent definitions and processes, systematic and random label noise, and low-quality or inappropriate inclusion of data. The medical sector is a case in point, with numerous unknowns, and new concepts arising over time. It also exemplifies another typical constraint—a very high cost for mistaken classification. A sensible way to tackle these situations is to build a model that flags confusing or unusual data samples requiring human intervention, while classifying acceptable data samples [1]. While this process is intuitively obvious to humans, neural networks behave abnormally in many cases, making overconfident mistakes when encountering confusing or unknown inputs [3], [5]. In this work, we build a multitask abstaining classifier for classifying the text pathology reports from the US National Cancer Institute SEER (Surveillance, Epidemiology, and End Results) registries [6] that simultaneously makes predictions on six tasks of interest to the registries: primary site (70 classes), histological type (547 classes), primary subsite (314 classes), laterality (7 classes), behavior (4 classes), and histological grade (9 classes) for a given text pathology report. We use an extra class, called the abstention class, for each task and train the model to learn the features for each class including the abstention class. Unlike existing approaches for abstention that are typically based on softmax thresholding methods [7] [8], our method learns features that lead to abstention, thus, allowing us to understand the reasons causing the confusion. We demonstrate how an abstaining classifier in a multitask setting can be used on real-world data to solve a complex problem and partially automate a human workflow, abstaining, *i.e.*, refusing to classify confusing samples, and thus requiring human intervention on these samples while making predictions on regular samples without a problem. We show that this is an intuitively simple yet very effective way of tackling inevitable errors when deploying machine learning models.

II. ABSTAINING CLASSIFIER IN A MULTITASK SETTING

A deep abstaining classifier [2], or DAC, introduced first for combating label noise, is basically a regular deep neural network classifier (DNN) but with an extra (abstention) class and a custom loss function that permits abstention during training. This allows the DNN to abstain on (or decline to classify) confusing samples while continuing to learn and improve classification performance on the non-abstained samples. The custom loss function for an abstaining classifier is a modified version of the standard cross-entropy and given by,

$$\mathcal{L}(x_j) = (1 - p_{k+1}) \left(- \sum_{i=1}^k t_i \log \frac{p_i}{1 - p_{k+1}} \right) + \alpha \log \frac{1}{1 - p_{k+1}} \quad (1)$$

where p_{k+1} is the probability of the abstention class and α is the penalty term for abstention.

This loss function behaves like a regular cross-entropy loss on the original classes and adds an additional loss, scaled by a tuning parameter α that controls the propensity of abstention. That parameter is selected during training to guarantee an upper bound on the abstention rate while optimizing the accuracy. The trade-off between accuracy and abstention rates is explored by re-optimizing the network for varying abstention rates.

Thulasidasan et al. [2] reported that the DAC can learn unlabeled features in the data which may be correlated with label noise. In practice, the label noise is a mix of both uncorrelated (e.g. labeling inconsistent with the report being classified) and correlated (e.g. ‘metastasis’ may indicate site labels are unreliable) so that perfect empirical identification of misclassified items can not be achieved. Since this is inherently dependent on the data, further discussion is deferred to the VI results section.

We modify the multitask convolutional neural network (MTCNN) model by Alawad et al. [9] to include abstention for each task. Their model uses a word-level CNN [11] [12] [15] [10] in a multi-task learning setting for automatic extraction of cancer information from unstructured text pathology reports to make predictions on 5 tasks: primary site (65 classes), laterality (4 classes), behavior (3 classes), histological type (63 classes), and histological grade (5 classes). Our model is an extension of their hard parameter sharing MTCNN where we train a model of similar architecture for six tasks (sub-site, in addition to the five previously listed) with a much higher number of classes per task.

The model diagram is shown in Figure 1 where we can see extra ‘abstain’ class for each of the tasks. The model has an embedding layer which represents each word token as a 300 dimensional word embeddings [13] [14]. These vectors are fed to three independent convolutional layers followed by one-dimensional max pooling layers, each with 300 filters (or feature maps) and filter sizes of 3, 4, and 5 respectively. The outputs of these max pooling layers are then concatenated and fed to six independent fully connected layers with softmax output (one for each task) which return the predictions for each individual task.

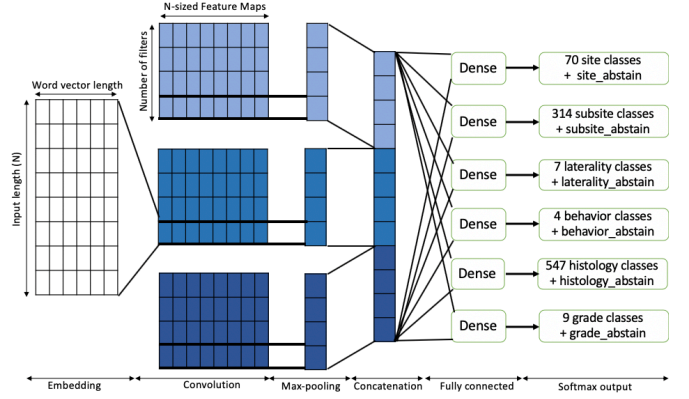


Fig. 1. Architecture of our model; the model is largely similar to [9] other than an extra task and the additional abstain classes for each of the tasks.

III. DETERMINANTS OF CLASSIFICATION WITH LIME

We used the Local Interpretable Model-agnostic Explanations (LIME) tool [4] to identify which words (in context) were most important (*pro* or *con*) in determining the final class assigned to each pathology report. LIME was provided with a trained DAC model and raw pathology reports. We used the text version of LIME, requesting the top 40 words-in-context relevant to identifying the winning class, using 100,000 perturbations, as described in the LIME documentation. These parameters resulted in a stable output, when comparing multiple runs on a sub-sample of the reports.

IV. DATASET DESCRIPTION

The study was done on a corpus of text cancer pathology reports from the Louisiana and Kentucky Tumor Registries. Each case of cancer (individual tumor), given by the case ID, is identified by a combination of a patient ID and a tumor ID. Ground truth for each case of cancer is obtained from the manually abstracted and consolidated records in the cancer registries. There are multiple reports for each case, each of which are identified by a combination of a patient ID, a tumor ID, and a report ID. The ground truth is consolidated for each case ID (*i.e.*, each individual tumor), meaning all the reports pertaining to a particular tumor has the same ground truth regardless of the content of the text pathology report.

V. EXPERIMENTAL SETUP

We train our abstaining classifier to achieve the following two goals that are desired by NCI and the cancer registries: i) a minimum of 97% accuracy for each task on the retained samples, ii) a maximum of 50% abstention, where abstention on one task implies abstention on all tasks. In case the model cannot achieve both, we prioritize retention over accuracy and report the achieved accuracy on the retained samples. The model is trained on the pathology reports from Louisiana and Kentucky SEER registries (approximately 320K reports) with training-validation-test split of 60-20-20%. After the training is done, using the validation set for setting the tuning parameters, we freeze all the parameters including α and evaluate the

model on the test data and report the scores on these data alone. We report the model accuracy and abstention rates on the 20% of the holdout test reports (untouched during training) from Louisiana and Kentucky registries. We further test the generalizability of the model across registries by reporting the accuracy and abstention of model prediction on pathology reports from Utah and New Jersey registries.

VI. RESULTS AND DISCUSSION

Table I shows for each task the base accuracy when the model is trained without abstention, the rate of abstention for the tuned α value, and the accuracy on the retained fraction of reports for all the four registries described in Sections IV and V. The test accuracy and rates of abstention for Louisiana-Kentucky are consistent with the ones on the train data. However, on New Jersey-Utah data, the accuracy scores are comparable but the abstention is slightly higher. This shows that the model generalizes well across different registries although at the cost slightly increased abstention when the input data looks different than what the model was trained on. The model achieves the desired accuracy of over 97% accuracy for the individual tasks of predicting behavior, site, and laterality with the constraint of the abstention rate below 50%. However, it fails to achieve the desired accuracy for the grade, histology, and subsite possibly because these are more complex problems with overlapping and changing definitions and have more problems in the training data.

Likewise, table II shows the joint base accuracy, abstention rates, and the accuracy on the retained samples for different combinations of the tasks. This facilitates evaluation of the model based on the priority of the desired combination of tasks. For any combination of tasks, a naïve guess for the accuracy and abstention rate would be the smallest of the individual accuracy and largest of the individual abstention rates, for example, for site-histology combination for LA-KY registries, the guess would be 90.27% accuracy with 38.75% abstention rate. However, this is possible only if the reports abstained by the model for the task with the highest abstention rate is the superset of the reports abstained by the model for the other tasks in the combination. Based on the results from the table II, we see that the model abstains on different sets of reports for different tasks, making the combined accuracy lower and the combined abstention higher than the naïve guess.

Figure 2 shows typical output from LIME for four specific reports. We can see from the correctly classified cancer types that the results returned by LIME make sense: ‘prostate’ is important when reports are correctly classified as prostate cancer, ‘lung’ for lung cancer, and ‘breast’ for breast cancer. Additionally, LIME provides other words one might not have anticipated, but that make sense after examining the context. For example, the subsite of breast tumors are often identified by analogy to a clock which is unique to breast cancers. The top word for breast cancer, ‘ductal,’ refers to a histology type, ‘ductal carcinoma,’ that is distinct to breast and pancreatic cancers. Similarly, lobes and lobectomies are distinct to lung cancers, and Gleason scores to prostate cancer. Also it is

TABLE I
ACCURACY OF BASELINE CLASSIFIER WITH NO ABSTENTION AND ABSTENTION RATE AND ACCURACY OF ABSTAINING CLASSIFIER ON RETAINED SAMPLES FOR INDIVIDUAL TASKS ON DATA FROM FOUR REGISTRIES.

Task	Louisiana - Kentucky			Utah - New Jersey	
	Base Acc (no abs)	Abs rate	Accuracy (retained)	Abs rate	Accuracy (retained)
Behavior	97.91%	0.00%	97.85%	0.00%	96.63%
Grade	76.71%	24.09%	83.35%	29.70%	78.20%
Histology	77.57%	38.75%	90.27%	47.36%	87.88%
Laterality	91.34%	43.94%	98.45%	48.19%	97.36%
Site	91.98%	24.46%	98.80%	28.90%	98.05%
Subsite	65.11%	20.41%	73.72%	21.72%	71.40%

TABLE II
ACCURACY OF BASELINE CLASSIFIER WITH NO ABSTENTION AND ABSTENTION RATE AND ACCURACY OF ABSTAINING CLASSIFIER ON RETAINED SAMPLES FOR DIFFERENT COMBINATION OF TASKS ON DATA FROM FOUR REGISTRIES. S: SITE, B: BEHAVIOR, H: HISTOLOGY, L: LATERALITY, G: GRADE

Task	Louisiana-Kentucky			Utah-New Jersey	
	Base Acc (no abs)	Abs rate	Accuracy (retained)	Abs rate	Accuracy (retained)
S.B	76.71%	24.46%	96.61%	28.90%	94.56%
S.H	90.06%	49.40%	90.20%	56.12%	87.88%
S.B,H	71.74%	49.39%	89.51%	56.12%	86.41%
S.B,L	83.78%	50.81%	95.64%	53.55%	93.87%
S.B,G	70.09%	40.77%	82.46%	47.68%	76.78%
S.B,H,L	67.14%	66.83%	90.06%	70.76%	88.55%
S.B,H,L,G	53.19%	72.24%	76.06%	76.45%	67.89%

frequently the case that reports correctly assigned to a cancer type have mostly positive contributors to the classification.

With the abstaining classifier, it is possible to identify those attributes of a report that suggest judgement should be withheld and the report placed in the ‘abstain’ class. In the example shown, the word stem ‘metast,’ ‘lymph,’ and ‘node’ are seen to be indicative of the abstention class, while words indicative of specific cancers weigh against the abstention class. In the case shown, the abstained report was associated with a breast cancer, and we can see that LIME is weighing the decision to abstain vs. choosing the breast cancer class. Also evident are several words that the DAC has evidently associated with abstention because of their association with metastasis: ‘metastatic’ and ‘primary.’ The ground truth available for training the DAC utilizes the annotations done by the SEER cancer registries, which assign reports to the original site of the cancer, so reports associated with metastasis are often difficult to correctly assign, and abstention is called for.

Our DAC was trained, validated, and tested on 320,000 pathology reports. This makes it difficult to assess general trends by hand. In Table III we attempt to quantify the extent to which particular reasoning extends across the data set, first by examining the frequency of words in the reports, and then by examining the frequency of LIME identification and the sign of the LIME coefficient. We observe that ‘breast,’ ‘lung,’

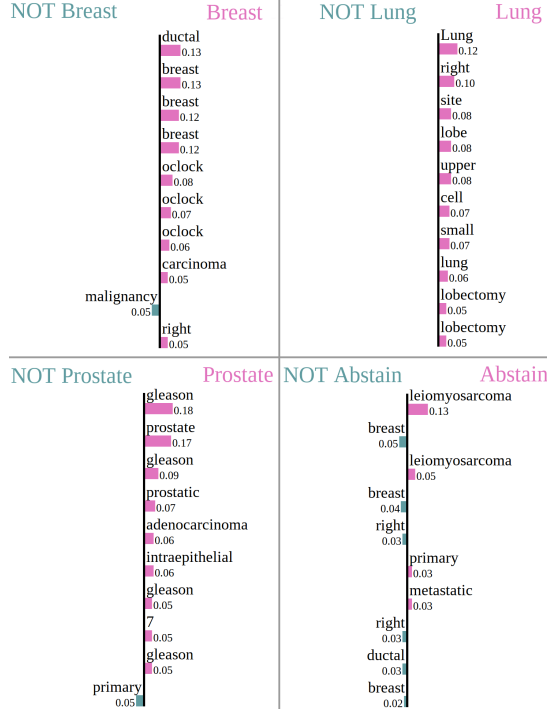


Fig. 2. Typical LIME output for four pathology reports classified with the DAC. The top ten word instances contributing to the indicated classification as assessed by LIME, together with the assigned coefficient. Positive coefficients are indicated by magenta bars to the right of center, while negative coefficients are in blue-green, and they are ordered with most important words at the top. Not shown, but provided by LIME is the context of each contributing word.

and ‘prostate’ are associated with correctly classified reports of their respective type. Column 9 of Table III provides the significance of association of each word with the abstention class. Examination of the LIME results provides two more metrics of importance of keywords when they occur, and we can see from column 10 of Table III. Cancer-specific terms are, not surprisingly, associated with reports correctly classified by site, rather than assigned to the abstention class.

Armed with this better tool, we see that the occurrence of the word stem ‘metast’ is less significantly associated with the abstention class than LIME-derived metrics. By combining the fraction of reports with each word and the fraction of time LIME associates these words with the abstention class, we can estimate the fraction of time metastasis is responsible for the abstention. For breast cancer, ‘metast’ is in 53% of the abstained reports, is identified by LIME as important for abstention 77% of the time, with the appropriate sign 65% of the time, suggesting metastasis is responsible for abstention roughly $0.53 \times 0.77 \times 0.65$, or 26% of the time. Similar reasoning suggests metastasis is responsible for 26% and 62% of the lung and prostate cancer abstentions, respectively.

Other reasons for abstention, besides metastasis, may include assays of lymph nodes, multiple samples described in the report, or simple lack of information, and will require more analysis to identify. Table III shows statistically significant associations are present for a variety of keywords.

TABLE III

ASSOCIATION OF WORDS WITH CLASS CHOICES OF OUR DAC. FOR THE CANCER TYPE IN COLUMN 1 AND THE WORD IN COLUMN 2, WE PROVIDE IN COLUMNS 3 AND 4 THE NUMBER AND PERCENTAGE OF REPORTS WITH A GIVEN WORD WHEN THE REPORT IS CORRECTLY CLASSIFIED AND WHEN THE REPORT IS ASSIGNED THE ABSTENTION CLASS. IN COLUMNS 5-6 AND 7-8, WE PROVIDE THE NUMBER AND PERCENTAGE OF THE REPORTS WITH THE WORDS WHERE LIME PICKED UP THE WORD AND WHEN THE COEFFICIENT FOR THE WORD WAS POSITIVE FOR CORRECTLY CLASSIFIED AND ABSTAINED REPORTS. COLUMN 9 IS THE P-VALUE FOR WORD OCCURRENCE DISTINGUISHING ABSTAINING AND CORRECT SITE CLASS USING 2x2 FISCHER’S EXACT TEST. COLUMN 10 IS THE P-VALUE FOR LIME IDENTIFYING, AND SIGN OF LIME COEFFICIENT IN DISTINGUISHING ABSTAINING CLASS FROM CORRECT SITE IDENTIFICATION WITH A 3x2 FISCHER’S EXACT TEST. \diamond , $*$, AND \ddagger INDICATE SIGNIFICANCE RANGE.

Site (corr/abs)	Word	Word in Report		Word Highlighted by LIME #(%)		Occur. p-value	LIME pickup p-value	
		Corr. #(%)	Abst. #(%)	Corr. ID	Positive ID			
Breast (320/320)	cancer	157(49)	66(25)	40(25)	22(55)	35(53)	31(88)	4.5e-14 \ddagger
	metast	155(48)	171(53)	38(24)	15(39)	131(77)	85(65)	2.3e-1
	primary	101(32)	118(37)	71(70)	7(10)	91(77)	54(59)	1.8e-1
	lymph	245(77)	178(56)	28(11)	25(89)	121(68)	51(42)	2.9e-8 \ddagger
	node	194(61)	150(47)	70(36)	58(83)	113(75)	8(7)	6.4e-4 \diamond
	origin	24(8)	61(19)	3(12)	1(33)	36(59)	8(22)	2.1e-5 \ddagger
Lung (320/320)	breast	320(100)	209(65)	293(92)	218(74)	206(99)	15(7)	6.9e-39 \ddagger
	malignan	104(33)	140(44)	39(38)	33(85)	110(79)	70(64)	4.3e-3
Prostate (320/320)	cancer	55(17)	49(15)	22(40)	19(86)	18(37)	14(78)	5.9e-1
	metast	128(40)	207(65)	86(67)	15(17)	168(81)	78(46)	5.5e-10 \ddagger
	primary	107(33)	103(32)	92(86)	23(25)	90(87)	54(60)	8.0e-1
	lymph	141(44)	103(32)	27(19)	11(41)	62(60)	37(60)	2.5e-3
	node	113(35)	79(25)	22(19)	22(100)	42(53)	18(43)	4.3e-3
	origin	82(26)	93(29)	68(83)	25(37)	55(59)	13(24)	3.7e-1
	tung	294(92)	146(46)	294(100)	294(100)	145(99)	84(58)	4.9e-39 \ddagger
	malignan	140(44)	197(62)	64(46)	21(33)	127(64)	39(31)	8.8e-6 \ddagger
Prostate (320/320)	cancer	152(48)	108(34)	100(66)	97(97)	55(51)	39(71)	5.2e-4 \diamond
	metast	107(33)	172(54)	54(50)	3(6)	116(67)	75(65)	3.0e-7 \ddagger
	primary	151(47)	75(23)	149(99)	0(0)	61(81)	25(41)	4.2e-10 \ddagger
	lymph	188(59)	156(49)	12(6)	10(83)	71(46)	50(70)	1.3e-2
	node	135(42)	127(40)	18(13)	4(22)	42(33)	23(35)	5.7e-1
	origin	12(4)	61(19)	3(25)	1(33)	51(84)	32(63)	5.9e-10 \ddagger
	prostate	320(100)	251(78)	320(100)	320(100)	242(96)	200(83)	5.5e-23 \ddagger
	malignan	112(35)	123(38)	107(96)	1(1)	88(72)	28(32)	4.1e-1
								2.7e-10 \ddagger

VII. CONCLUSION

We used a deep abstaining classifier to identify six attributes of cancers, by processing associated pathology reports. By including an explicit abstention class, we were able to greatly increase the accuracy of classification on non-abstained reports. Furthermore, we showed, quite plausibly, through application of LIME, that reports were abstained when concepts such as metastasis or lymph nodes were positively associated with the abstention class. Identification of the determinants of abstention should facilitate our ability to use the DAC in a real-world setting.

VIII. ACKNOWLEDGEMENTS

This work has been supported in part by the Joint Design of Advanced Computing Solutions for Cancer program established by the US Department of Energy and the National Cancer Institute of the National Institutes of Health. This work was performed under the auspices of the US Department of Energy by Argonne National Laboratory under contract DE-AC02-06-CH11357, Lawrence Livermore National Laboratory under contract DE-AC52-07NA27344, Los Alamos National Laboratory under contract DE-AC5206NA25396, and Oak Ridge National Laboratory under contract DE-AC05-

00OR22725. This research was supported by the Exascale Computing Project (17-SC-20-SC), a collaborative effort of the US Department of Energy Office of Science and the National Nuclear Security Administration.

REFERENCES

- [1] Nicolas Hengartner, Leticia Cuellar, Xiao-Cheng Wu, Georgia Tourassi, John Qiu, Blair Christian, Tanmoy Bhattacharya, "CAT: computer aided triage improving upon the Bayes risk through ϵ -refusal triage rules", BMC bioinformatics, Vol 18, pp 3-8.
- [2] Sunil Thulasidasan, Tanmoy Bhattacharya, Jeff Bilmes, Gopinath Chennupati, and Jamal Mohd-Yusof, "Combating Label Noise in Deep Learning Using Abstention", Proceedings of the 36th International Conference on Machine Learning, 2019.
- [3] Sunil Thulasidasan, Gopinath Chennupati, Jeff Bilmes, Tanmoy Bhattacharya, and Sarah Michalak, "On Mixup Training: Improved Calibration and Predictive Uncertainty for Deep Neural Networks", Proceedings of the Thirty-third Conference on Neural Information Processing Systems (NeurIPS 2019), December 2019.
- [4] Marco Tulio Ribeiro, and Sameer Singh, and Carlos Guestrin, "Why Should I Trust You?: Explaining the Predictions of Any Classifier" 22nd ACM SIGKDD, 2016.
- [5] Anh Nguyen Jason Yosinski, and Jeff Clune, "Deep neural networks are easily fooled: High confidence predictions for unrecognizable images", Proceedings of the IEEE Conference on Computer Vision and Pattern Recognition, pp.427–436, 2015.
- [6] National Cancer Institute at National Institutes of Health, "What is SEER?", <https://www.cancer.gov/research/areas/public-health/what-is-seer-infographic>, 2015.
- [7] Dan Hendrycks, and Kevin Gimpel, "A baseline for detecting misclassified and out-of-distribution examples in neural networks", arXiv preprint arXiv:1610.02136, 2016.
- [8] Abhijit Bendale, and Terrance E Boult, "Towards open set deep networks", Proceedings of the IEEE conference on computer vision and pattern recognition, 2016.
- [9] Mohammed Alawad, Shang Gao, John X Qiu, Hong Jun Yoon, J Blair Christian, Lynne Penberthy, Brent Mumphrey, Xiao-Cheng Wu, Linda Coyle, and Georgia Tourassi, "Automatic extraction of cancer registry reportable information from free-text pathology reports using multitask convolutional neural networks", Journal of the American Medical Informatics Association, vol. 27, pp. 89 – 98, 2020.
- [10] Yoon Kim, "Convolutional Neural Networks for Sentence Classification", Proceedings of the 2014 Conference on Empirical Methods in Natural(EMNLP), publisher ACL, pp. 1746–1751, April 2014.
- [11] Ken. Chatfield, Karen Simonyan, Andrea Vedaldi, and Andrew Zisserman, "Return of the devil in the details: Delving deep into convolutional nets", In Proceedings of the British Machine Vision Conference (BMVC), 2014.
- [12] Alex Krizhevsky, Ilya Sutskever, and Geoffrey E. Hinton, "Imagenet classification with deep convolutional neural networks", Advances in neural information processing systems (NIPS), pages 10971105, 2012.
- [13] Tomas Mikolov, Ilya Sutskever, Kai Chen, Greg Corrado, and Jeffrey Dean, "Distributed Representations of Words and Phrases and their Compositionality", Advances in neural information processing systems (NIPS), 2013.
- [14] Tomas Mikolov, Kai Chen, Greg Corrado, and Jeffrey Dean, "Efficient Estimation of Word Representations in Vector Space", International Conference of Learning Representations (ICLR) workshop, 2013.
- [15] Christian Szegedy, Wei Liu, Yangqing Jia, Pierre Sermanet, Scott Reed, Dragomir Anguelov, Dumitru Erhan, Vincent Vanhoucke, and Andrew Rabinovich, "Going deeper with convolutions", Computer Vision and Pattern Recognition (CVPR), 2015 IEEE Conference on IEEE, 2015.